Case-PDM Optimized Compressed Sensing Sampling for Fat-Water Separation

S. Narayan[1], J. Miao[1], F. Huang[1], D. Johnson[2], G-Q. Zhang[1], and D. Wilson[1]
[1]Case Western Reserve University, Cleveland, OH, United States, [2]Ohio State University, Columbus, OH, United States

Introduction

Compressed sensing (CS) can be used to generate source data for chemical shift imaging decomposition algorithms[1]. The undersampling allowed by CS can greatly reduce the lengthy scan times necessary to acquire the multiple images, typically at least three, used in decomposition algoirhtms[2]. However, the distribution of CS undersampling among the three source images has not yet been optimized. For example, to achieve a given global sampling ratio (the number of lines of k-space used in the CS reconstructions divided by the number of lines available in a full resolution data set), we do not know whether it is better to sample all three source images uniformly, or if it is better to sample one of the images more than the others. A perceptual difference model (Case-PDM), which has been successfully applied to optimize keyhole, spiral, SENSE, GRAPPA, and CS algorithms[3-6], was used as the basis of comparison for optimizing the CS sampling because the model is able to sensitively detect reconstruction artifacts that could arise from CS undersampling and processing. The purpose of this study is to find the distribution of samples among the three source images that yields decompositions that are perceptually closest to a fully sampled reference.

Methods

We first restricted our SRs for each source image to one of the following seven values: 0.4, 0.5, 0.6, 0.7, 0.8, 0.9, and 1. We used variable density (VD) strategy to create undersampled data with the center of k-space sampled more than other regions[6]. We specified a global SR, and generated all of the possible permutations of individual SRs, using only the sampling ratios enumerated above, for that specified global SR. For example, this includes the uniform scheme (e.g.: for a global ratio of .5, each of the source images has a SR of .5), and sampling one of the source images more while compensating by further undersampling the other source images (e.g.: for a global ratio of .5, one source image has a SR of 0.7, and the others have a SR of 0.4).

We then used Case-PDM, a perceptual difference model, to compare the decompositions sourced from the undersampled data to a set of fully sampled reference decomposition. We used Case-PDM to compare the water and fat parameter maps that arise from our accelerated VARPRO-ICM algorithm (presented separately). Summing the two PDM scores (one each for the water map and fat map) gave a quantitative image quality metric suitable for comparing undersampling schemes. The scheme with the lowest Case-PDM score was determined optimal for a given global SR.

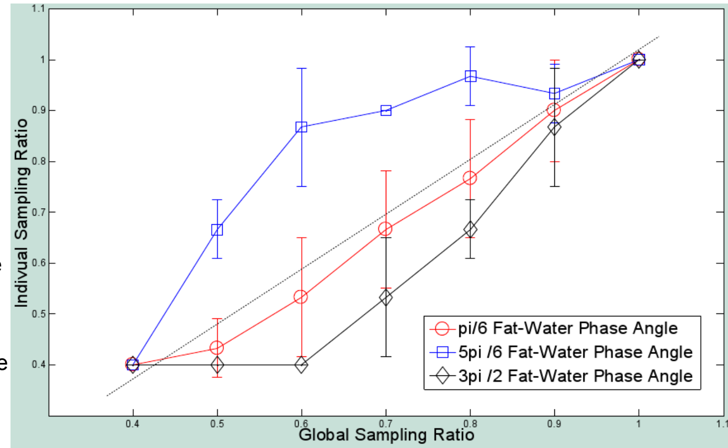

Figure 1: *Case-PDM Optimized Sampling Ratio (SR) Distributions.* For each given global SR (equal to the average of the three individual sampling ratios), the optimal distribution of individual SRs among the source images was found. From the plot, we can see that the optimal way to distribute samples is not equally among the three source images. Rather, it was consistently more important (in terms of perceptual differences) to sample at a fat-water phase difference of 5π/6 than at an angle of π/6, which was in turn more important than sampling at an angle of 3π/2. The error bars represent fluctuation of individual optimal SRs across 3 mouse data sets.

Results

The PDM score for both the water and fat maps decreases in proportion to increases in global SR. At a global SR of 100%, a zero PDM score is obtained. An imperceptible PDM score can obtained at global SR of 0.9.

For each global SR, the optimal set of individual SRs was found, which is shown in Figure 1. We consistently found that the optimal way to distribute samples was to sample the 5π/6 scan more than the π/6 scan, which, in turn, should be sampled more than the 3π/2 scan. With this sort of sampling scheme, we could achieve a fat/water decomposition that was perceptually closest to the reference decomposition. The errors bars in Figure 1 represent variation in the optimal sampling scheme between animals. A comparison of uniformly and optimally sampled decompositions are shown in Figure 2. The results show that using the uniform sampling scheme causes more aliasing artifacts in the decomposition than does using the optimal sampling scheme.

Figure 2: *Comparison of Uniform and Optimal Sampling Schemes at .7 Global Sampling Ratio.* The three water decomposition images above are sourced from a: a) fully sampled data set, b) uniformly distributed data set (i.e., individual SRs of .7, .7, and .7), and c) optimally distributed data set (i.e., .8, .9, and .4 SRs for π/6, 5π/6 and 3π/2 images, respectively). As demonstrated by areas labeled by the white arrows, the optimal sampling scheme leads to decompositions that perceptually closer to the reference image than does the uniform sampling scheme. Case-PDM scores for images (b) and (c), relative to (a), were: 6.13 and 5.12, respectively.

Discussion

We have experimentally shown that the optimal way to distribute CS sampling among the three source images necessary for our accelerated VARPRO-ICM algorithm is not to uniformly distribute the samples among the three source images. Using the scheme described above, we can generate water and fat parameter maps that are perceptually closest to the decompositions that are from a fully sampled reference data set. Our results showed that the distribution of samples among different chemical shift-weightings should be ranked as 5π/6 more than π/6, more than 3π/2 for optimal perceptual performance, but we have not yet fully explored this quantitatively. One possible explanation for our result is that the 5π/6 image has the largest difference in phase between fat and water, which might imply that this is the most important image for fat-water decomposition. More work still needs to be done before this can be definitively explained.

Acknowledgments
Award Number F30DK082132 from the NIDDK, NIH grant T32GM07250 to the Case MSTP from the NIGMS, NIH K25EB004467, Ohio Biomedical Research and Technology Transfer award, "The Biomedical Structure, Functional and Molecular Imaging Enterprise," Research Facilities Improvement Program Grant Number C06 RR12463-01 from the NCRR, and SAIRP grant EB004070. The content is solely the responsibility of the authors and does not necessarily represent the official views of the NIDDK, NIGMS, NCRR, or the NIH.

References

[1] Lustig, M. et al. ISMRM 2009; *17*:2646.[2] Hernando, D., et al. MRM 2008; *59*:571-580.[3] Salem, K.A., et al., Journal of Electronic Imaging, 2002; *11*:224.[4] Huo, D., et al., JMRI 2008; *27*:1412-1420.[5] Miao, J., et al., Medical Physics 2008; *35*:2541-2553[6] Miao, J., et al. ISMRM 2009; 17:3999.